J Therm Anal Calorim (2015) 122:1331–1339
DOI 10.1007/s10973-015-4875-7

The investigation of flammability, thermal stability, heat resistance and mechanical properties of unsaturated polyester resin using AlPi as flame retardant

Youchuan Wang[1] · Le Zhang[1] · Yunyun Yang[1] · Xufu Cai[1]

Received: 20 December 2014 / Accepted: 15 June 2015 / Published online: 3 July 2015

Abstract The influence of aluminum dialkylphosphinate (AlPi) on the flammability, thermal properties and mechanical properties of unsaturated polyester resins (UPRs) was investigated. A series of flame-retarded UPR loading with AlPi were prepared. The flammability and thermal stability of these UPR composites were investigated with limiting oxygen index (LOI), UL-94 vertical burning and themogravimetric analysis test. The structure and morphology of char residues were examined with Fourier transform infrared and scanning electron microscopy (SEM). Additionally, thermomechanical property of cured composites was characterized by dynamic mechanical analysis (DMA). The results showed that the AlPi excellently improved the flame retardancy of UPR, the LOI increased from 21 to 29.5 with the increasing of AlPi and UPR-AlPi25 (25 %) passed V-0 classification. The char residue of UPR-AlPi25 at 700 °C was 11.17 % in nitrogen and 20.83 % in oxygen, suggested that interaction between AlPi and UPR strengthened the char-formation ability and the thermal stability of the UPR/AlPi systems. The SEM showed that the surface of the char for UPR-AlPi25 was strong and dense and flexural fracture surfaces of UPR/AlPi composites showed a homogeneous morphology. The DMA curve indicated the T_g was greatly improved with the increasing of AlPi.

Keywords Unsaturated polyester resin · Flame retardance · Thermal stability · Aluminum dialkylphosphinate

✉ Xufu Cai
caixf2008@scu.edu.cn

[1] Department of Polymer Science and Engineering, Sichuan University, Chengdu 610065, China

Introduction

Unsaturated polyester (UP) resins are pre-polymer mixtures of unsaturated polyester chains and styrene with the latter serving as both a diluent and crosslinking agent during the subsequent radical curing process, which is one of the most versatile classes of thermosetting polymers. Due to their low raw materials and production costs, they have easy processing and excellent mechanical performance, electricity performance and chemical resistance [1, 2], which is widely used alone or in fiber-reinforced composite industry in the field of naval construction, offshore applications, coatings, building construction, automotives, etc. [3, 4]. However, typical UPR has both very weak resistances to fire and high smoke densities during burning because of its intrinsic chemical composition and molecular structure. The high flammability of UPR limits its further application in some areas, e.g., in the electrical industry [5]. So their increasing commercial utilization demands the development of flame retardant systems to reduce fire hazards.

Flame retardant is a kind of chemical additives, which can inhibit the process of fuel combustion and even make the burnable fuel noncombustible. But now used by most of the flame retardants on the market for compounds containing halogen and when halogen-containing resins burn, they generate smoke and toxic fumes, which can be expected to result in environmental problems. In order to protect the environment and human health, researchers have focused on developing effective halogen-free flame retardants.

Recently, phosphorus-containing compounds, as halogen-free flame retardants, have received considerable attention [6–8]. Generally, there are two methods used to prepare phosphorus UPR composites. One is to add

nonreactive phosphorus-containing flame retardant additives into UPR during processing [9]. It is reported that UPR can be modified with ammonium polyphosphate, melamine pyrophosphate [10], red phosphorus [11] and DOPO ramification [12] to improve their flame retardancy. Another way is by adding reactive phosphorous compounds reacting with UPR to introduce phosphorus into the polymer chain. Fong [13] had synthesized hexa-allylamino-cyclotriphosphazene (HACTP) as a reactive fire retardant for UPR, and Ma et al. [14] had synthesized spirocyclic pentaerythritol di(phosphoric acid monochloride)s (SPDPC)as a new monomer being introduced to the polyester. A novel reactive phosphorus-containing acrylate (ODOPB-AC) was synthesized and has been introduced into UPR successfully [5].

Dialkylphosphinate salt belongs to a new class of additive-type phosphorus-containing fire retardants. The key aspects of these salts are their high phosphorus content ($\sim$17 %). In particular, no harmful and toxic substances are released during combustion, so they have potential applications in E&E products [15]. The roles of dialkylphosphinic salts in reducing flammability of polymers are related to the structure of alkyl and metal, as well as the chemical structure of the polymer matrix and interaction with other additives [16–18]. Aluminum dialkylphosphinate is one of the most commonly used hypophosphite, which has been widely used in PET, PA6, PA66, EP [19–20].

In this article, aluminum dialkylphosphinate (AlPi) was used as flame retardants for UPR. The aim of the current research is to investigate the impact of AlPi on unsaturated polyester performance. The formulations in this study will be reviewed for the curing process of UPR with AlPi by DSC, the compatibility of AlPi and UPR by SEM. The results for residues morphology by SEM and structure by FTIR spectra, thermogravimetric analysis, fire performance using LOI and UL94 and ,furthermore, heat resistance by DMA, mechanical analysis will be described and discussed.

Experimental

Materials

The material used in this study is aluminum diethylphosphinate (Exolit AlPi supplied by Clariant). Maleic anhydride (MA), phthalic anhydride (PA), 1,2-propanediol (PG), styrene (St), hydroquinone (HQ), ethylene glycol, diethylene glycol, dimethylbenzene, zinc acetate were obtained from Chengdu Kelong Chemical Reagent Factory (China). Methyl ethyl ketone peroxide (MEKP) was supplied by Union Chemical Works Ltd (Taiwan). Co was supplied by Great Lakes Chemical Co (USA).

The synthesis of unsaturated polyester

The UPR was prepared by one-stage process. In a 500-mL four-necked round-bottom (RB) flask equipped with a mechanical stirrer, thermometer and nitrogen inlet, diols, MA and PA were taken in the molar ratio 1.1:0.5:0.5. A slight excess of diols (10 %) was provided to allow for evaporation losses. The molar ratio of 1, 2-propanediol, ethylene glycol and diethylene glycol is 6:3:1. In addition, 0.4 % of zinc acetate was added as catalyst. Air was exhausted and the mixture was heated in an oil bath slowly. Stirring started when the materials reached a semi-molten, then ascended to 160 °C, began to reflux, esterification started at this temperature. After keeping the temperature about 4 h, the condenser water was reduced, and the acid value was about 140 mg KOH g^{-1}; changing the device, installing water knockout drum, 10 % of xylene was added as dehydration agent in order to bring out the water generated in the esterification, heated up to 190–200 °C, until the acid value below 25 mg KOH g^{-1}; the reaction was completed and nitrogen gas was stopped, then a vacuum pump was used for 1 h, and the heating was stopped. When the temperature dropped to 160 °C, inhibitor hydroquinone (0.02 % of the total resin mass) was added, and stirring continued until the temperature dropped to 120 °C; added to crosslink agent of styrene (35 % of the total resin mass), stirred for 20 min and obtained pale yellow UPR.

Curing procedure of the UPR/AlPi blends

Filler (AlPi) with different content was added to UPR at room temperature. The mixture was stirred with a mechanical stirrer for 20 min and then dispersed through ultrasonication technique (700 W) during 20 min. An appropriate amount of MEKP and Co (UPR/MEKP/CO = 100/1/0.5, m/m/m) were then added to the mixture to obtain a homogeneous solution by several minutes of mechanical stirring. After degasification, the prepared mixture was poured in the mold for curing and post-curing at oven as the following procedure: 45 °C/2 h + 90 °C/2 h + 120 °C/2 h. The formulations are summarized in Table 1.

Characterization

The Netzsch Q-200 was used for differential scanning calorimetry (DSC) under nitrogen atmosphere using a scanning rate of 10 K min^{-1}. The compatibility of AlPi and UPR and the morphologies of the surface of the char obtained after the LOI test were observed by using Inspect-F SEM. Thermogravimetric analysis (TG) tests were carried out by the TG (Netzsch TG209) at a linear heating rate of

Table 1 Results of UL94 and LOI tests for neat UPR and its composites

Specimen	Composition/mass%				*P* content /mass%	LOI/%	UL-94
	UPR	AlPi	MEKP	Co			
UPR	100	0	1	0.5	0	21	NR[a]
UPR-AlPi5	95	5	0.95	0.475	1.19	25	NR
UPR-AlPi10	90	10	0.9	0.45	2.38	27	NR
UPR-AlPi15	85	15	0.85	0.425	3.57	27.5	V-2
UPR-AlPi20	80	20	0.8	0.4	4.76	28	V-1
UPR-AlPi25	75	25	0.75	0.375	5.95	29.5	V-0

[a] No rating

10 K min^{-1} and a flow of 60 cm^3 min^{-1} under pure nitrogen and air with the temperature range from 30 to 700 °C. The samples mass was 5–10 mg. LOI data of all samples were obtained at room temperature on an oxygen index instrument (XYC-75) produced by Chende Jinjian Analysis Instrument Factory, according to GB/T2406-93 standard. The dimensions of all samples were 130 × 6.5 × 3 mm^3. The FTIR spectra of the char residues were recorded on a Nicolet Magna-IR 560 spectrometer (Nicolet Instrument Co, USA) with KBr plate technique.

Results and discussion

Curing process of UPR with AlPi

Under certain conditions, heat of polymerization is a measure of the curing reaction activity and a sign of curing capability. By the higher curing reactivity, the higher exothermic peak, exothermic reaction characteristic curve, we can understand the reaction characteristics of UPR. Figure 1 shows the dynamic DSC curves of curing reactions from 20 to 220 °C of neat UPR and various UPR/AlPi mixtures. Compared with sharp exothermic peak of pure UPR, the exothermic peak of UPR/AlPi mixtures is flatter and wider. Simultaneously, the heat flow and exothermic peak temperature of UPR with AlPi are lower and indicate adding AlPi makes the exothermic temperature range widened and heat release rate slowed down. This is advantageous to the mechanical properties of the resin, because exothermic peak temperature is too high, due to polymer poor heat conductivity, which will cause internal thermal stress, prone to warping and cracking. Otherwise, not only pure resin but also the resin contained AlPi have two exothermic peaks: The first one is the main peak, which is generated by the normal flow of the resin; heat release is larger, and the second is post-cured exothermic peak. But the post-cured exothermic peak of mixtures with AlPi is not obvious, which are overlapped with the main

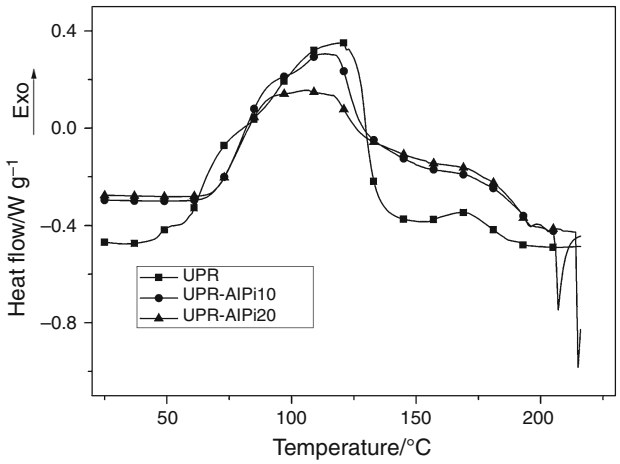

Fig. 1 DSC curing exotherm of UPR and UPR/AlPi composites in N_2

peak. This is due to the pure resin fast heat release leading to the formation of crosslinked networks prematurely, which makes movement of molecular chain blocked and only be initiated at higher temperature, so post-curing is obvious, while the main peak of mixtures with AlPi is lower from Fig. 1, so the crosslinked networks do not form instantaneously and the curing is more complete in main exothermic stage, resulting in unobvious post-cured exothermic peak due to fewer unreacted double bonds.

Flammability

LOI is an important parameter for evaluating the ease of extinguishment of polymeric materials in the same condition. It denotes the lowest volume concentration of oxygen sustaining burning of materials in the mixing gases of nitrogen and oxygen [21]. LOI and UL-94 results are given in Table 1, which shows that a significant increase in LOI (from 21 to 29.5) was observed when AlPi was utilized in the UPR composites. This reveals that the addition of AlPi is effective in promoting flame retardance of UPR.

However, UPR, UPR-AlPi5 and UPR-AlPi10 cannot pass the minimum classification of the UL-94 test, UPR-AlPi15 only pass the V-2 classification, and UPR-AlPi25 is capable of passing the V-0 classification.

Thermal analysis

The TG and DTG curves for AlPi, cured pure UPR and various UPR/AlPi mixtures under nitrogen and air are shown in Figs. 2 and 3. In nitrogen, the degradation of AlPi occurs in a single step from 400.8 ($T_{5\%}$) to 520 °C with a maximum degradation rate at 473.5 °C (T_{max}). The pyrolysis mechanism of AlPi was already reported [22]. The AlPi first degrades leading to the formation of some carbonaceous char and aluminophosphonate composed of octahedral aluminum and phosphonate groups. The phosphorus compound then decomposes in a transitory aluminum phosphonate which then turns into anamorphous aluminophosphate ($AlPO_4$) [23]. During the decomposition of AlPi, it was demonstrated that AlPi could partially sublimate and/or that ethane and diethylphosphinic acid are

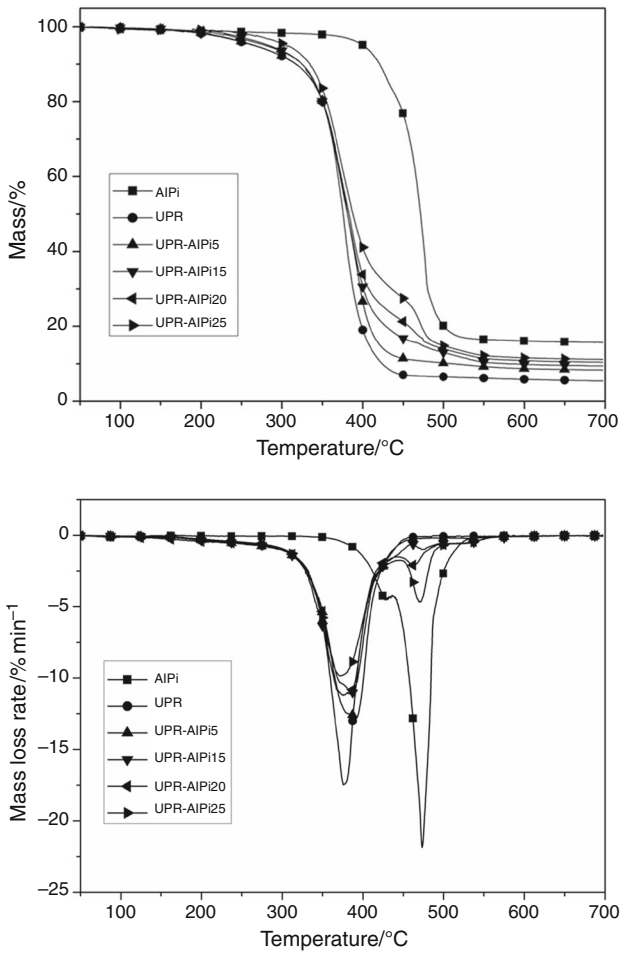

Fig. 2 TG and DTG curves of finally cured products in N_2

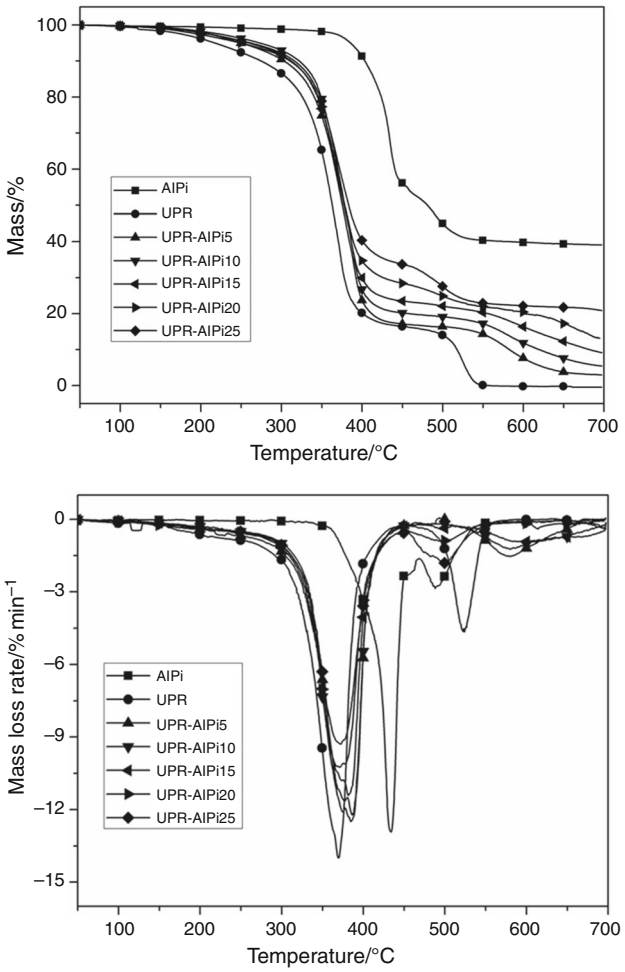

Fig. 3 TG and DTG curves of finally cured products in air

released [24]. At 700 °C, the final residue of 15.74 % is composed of condensed carbonaceous structures coming from the condensation of the products resulting from the degradation of the diethyl part of AlPi and crystallized aluminophosphates [23]. The $T_{5\%}$ of pure UPR is lower than that of UPR/AlPi composites in Tab.2 owing to the higher initial decomposition temperature of AlPi. The degradation of pure UPR and UPR-AlPi5 also occurs in a single step, and temperature of maximum rate of mass loss (T_{max}) was 376.1 and 391.7 °C separately. However, UPR/AlPi composites showed two-stage decomposition processes, and more and more obvious with the increasing of AlPi from 15 to 25 %. The first stage is from 270 to 450 °C, and corresponding T_{max} is about 370–380 °C, which is consistent with the T_{max} of pure UPR, and the second stage is from 450 to 500 °C, and corresponding T_{max} is about 460–470 °C, which is also consistent with AlPi. This means that the dispersing effect between AlPi and UPR has certain reduced with the increase in the content of AlPi. Starting from UPR-AlPi15, some cumulate

AlPi was decomposed in decomposition temperature of AlPi to produce the second peak, which is consistent with the accumulation phenomena observed in SEM (Fig. 8c–d). In Table 2, char yield of pure UPR and AlPi at 700 °C is only 5.42 and 15.74 %; the residue of UPR/AlPi composites was increased from 8.34 to 11.17 % with the increasing of AlPi and indicates that AlPi provides a tendency for remarkable flame retardance and char formation. AlPi may degrade leading to the formation of aluminophosphate, which protects the UPR substrate, and improve the content of char residue.

While under air (Fig. 3), compared with the results obtained in N_2, AlPi shows two distinct steps of mass loss between 350 and 500 °C and forms a residue of about 39 % at 700 °C. This result is consistent well with that reported by Lorenzetti [25]. The decomposition of AlPi in air leads to more residue than in N_2. In air, the decomposition begins at lower temperature, which suggests that AlPi is sensitive to oxygen during pyrolysis. The phosphinates are totally oxidized at 425 °C, and they cannot be vaporized since it occurs at a temperature between 425 and 480 °C, so phosphonates, pyrophosphates and phosphates were formed before ascended to 500 °C, while under nitrogen, these products only appeared at 500 °C [26], so phosphinates will evaporate in N_2 and lead to less residue.

TG and DTG curves for the UPR/AlPi composites from 5 to 25 % of filler loading and pure UPR under air are shown in Fig. 3. Their results are listed in Table 3. The whole degradation course of composites and pure UPR could be divided into two stages. For neat UPR, the amount of mass loss is about 80 % in the first stage from 210 to 400 °C, about 20 % in the second stage between 500 and 550 °C, almost no residue. But for the composites, the first-stage degradation occurred from 250 to 450 °C, the amount of mass loss is lower and lower with the increase in AlPi, which just like in the nitrogen, and the decomposition temperature of AlPi is higher. The second step is being very gradual compared to neat UPR. With dehydration and carbonization, the phosphorous group acted as a promoter to form heat-resistant char. The char might be oxidized at high temperature and leaded to further mass loss. But the second stage of UPR-AlPi5, UPR-AlPi10 and UPR-AlPi15 was occurred between 530 and 650 °C, while UPR-AlPi20 and UPR-AlPi25 was occurred between 450 and 550 °C. The T_{2max} (522.3 °C) of neat UPR is higher than that of AlPi (488 °C), so phosphonates, pyrophosphates and phosphates were formed before UPR was oxidized, which protected the UPR substrate and were good for the formation of residue. The presence of AlPi reduces total oxidation reaction. This effect is known for phosphorus polymer systems [27]. The results were consistent with the residue of various composites in Table 3 (from 3 to 20.83 %).

Figure 4 shows the experimental and theoretical TG curves of UPR-AlPi25 system in N_2 and air. The theoretical curve was calculated based upon the mass percentage of the ingredient in the UPR-AlPi25 system. As could be seen in N_2, when the temperature was below 400 °C, the experimental and theoretical curves were almost not different. However, the experimental residual char became more than the theoretical one after 400 °C. From Fig. 2, before 400 °C, the decomposition of UPR had almost completed before decomposition of AlPi, so aluminophosphonate produced by the decomposition of AlPi protected the UPR from further degradation after 400 °C. From Table 2, the DTG curves show that R_{max} of pure UPR and AlPi is 17.48 and 21.86, respectively, while UPR/AlPi composites were lower and lower with the increasing of AlPi and were lower than pure resin and AlPi, which suggested that the interaction between AlPi and UPR reduced the mass loss rate. While the experimental and theoretical TG curves of UPR-AlPi25 system in air were

Table 2 TG and DTG data under nitrogen condition for neat UPR and its composites with AlPi

Specimen	Temperature/°C			Y_c/%	R_{max}/% min^{-1}
	$T_{5\%}$	$T_{10\%}$	T_{max}		
AlPi	400.8	421.1	473.5	15.74	21.86
UPR	266	317.2	376.1	5.42	17.48
UPR-AlPi5	267.2	317.7	391.7	8.34	12.82
UPR-AlPi15	270.8	319.9	376/470	9.42	11.22/1
UPR-AlPi20	278.1	329.5	385.1/463.5	10.42	10.95/2.1
UPR-AlPi25	284.2	326.7	371.5/471	11.17	9.86/4.69

$T_{5\%}$—the temperature of 5 % loss decomposition (set $T_{5\%}$ as initial decomposition temperature), $T_{10\%}$—the temperature of 10 % loss decomposition, T_{max}—the temperature of the decomposition peak, Y_c—the char residues at 700 °C, R_{max}—the decomposition speed at the decomposition peak

Table 3 TG and DTG data under air condition for neat UPR and its composites with AlPi

Specimen	Temperature/°C			Y_c/%	R_{max}/% min^{-1}
	$T_{5\%}$	$T_{10\%}$	T_{1max}/T_{2max}		
AlPi	385	403.3	433.9/488	39.07	12.93/2.86
UPR	217	274.8	369.7/522.3	0	14/4.65
UPR-AlPi5	250.1	303.3	386.2/579.6	3	12.23/1.53
UPR-AlPi10	273.1	322	384.5/579.4	5.45	12.49/1.23
UPR-AlPi15	259.7	312.1	381.6/596.6	9.17	11.41/0.94
UPR-AlPi20	249.4	310.8	371.1/493.1	12.7	10.25/0.9
UPR-AlPi25	262	316.2	372.3/501.1	20.83	9.29/1.8

T_{1max}—represents the temperature of the first maximum mass loss rate for the system, T_{2max}—represents the temperature of the second maximum mass loss rate for the system

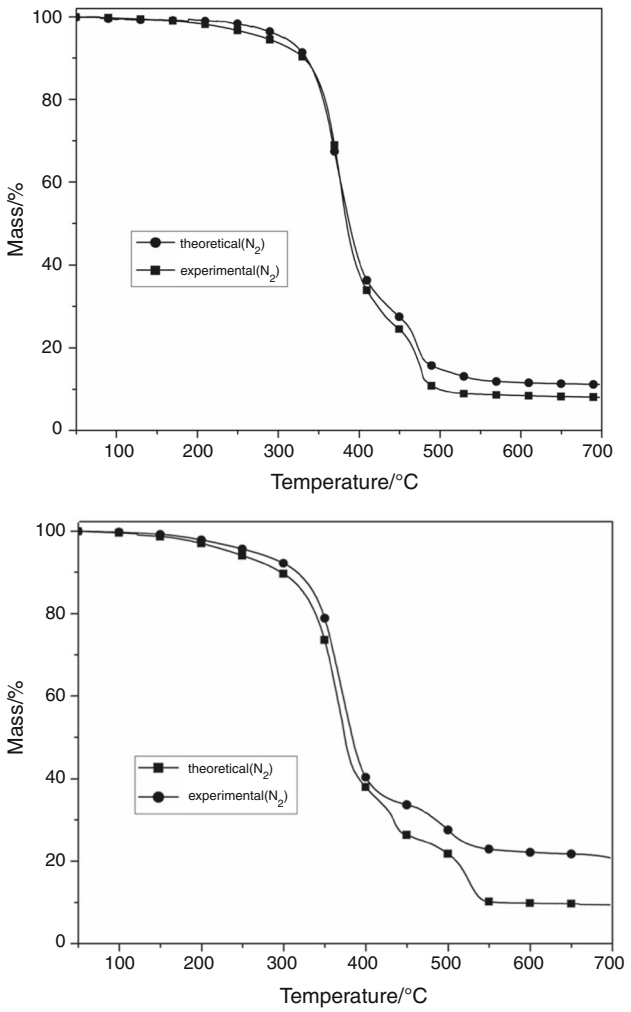

Fig. 4 Experimental and theoretical TG curves of UPR-AlPi25 system in N_2 and air

different, the experimental residual char became more than the theoretical one at the whole temperature range of UPR, and the theoretical curve showed three distinct steps of mass loss compared with two steps of experimental curve. It could be deduced some high-temperature stable material was produced in the char due to the interaction between AlPi and UPR.

Morphology of the residue char

To explore how the structure of char determines the flame retardancy of UPR, we investigated the char morphology left after LOI testing by SEM. Figure 5 presents SEM micrographs of UPR/AlPi and UPR residues. For neat UPR (Fig. 5a), the flammable gas released by the combustion of internal substrate makes carbon layer porous, which cannot block the air into the interior, so almost no residual carbon of pure resin in air. This poor residual carbon could not effectively protect the underlying UPR from degradation during combustion. Therefore, UPR cannot pass UL-94. However, the char surface of UPR composite, illustrated in Fig. 5b, was compact and tight. This structure of the char could prevent heat transfer between the AlPi and substrate and thus protect the underlying materials from further burning and pyrolysis, so they had much higher LOI. In addition, this char structure could offer a good shield to prevent UPR from burning, and this was proved in vertical flammability tests (Table 1).

Structural analysis of the combustion residue by FTIR

In order to further understand the chemical alteration in the condensed phase of flame retardant UPR composites, Fig. 6 shows the FTIR spectrum of cured UPR-AlPi25 and the residue obtained from LOI testing of UPR-AlPi25. For the cured UPR-AlPi25, the absorptions of –OH (3453.05 cm^{-1}), aromatic =C–H stretch (3027 cm^{-1}), aliphatic vibrations of C–H (2880–2958 cm^{-1}), aromatic ring (1632–1409 cm^{1}) and O=C–O (1731 cm^{-1}) were detected

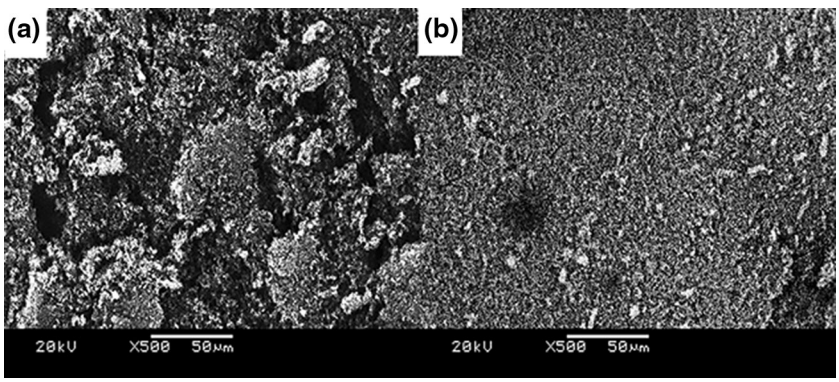

Fig. 5 SEM pictures of the residue after LOI testing of UPR (**a**) and UPR-AlPi25 (**b**)

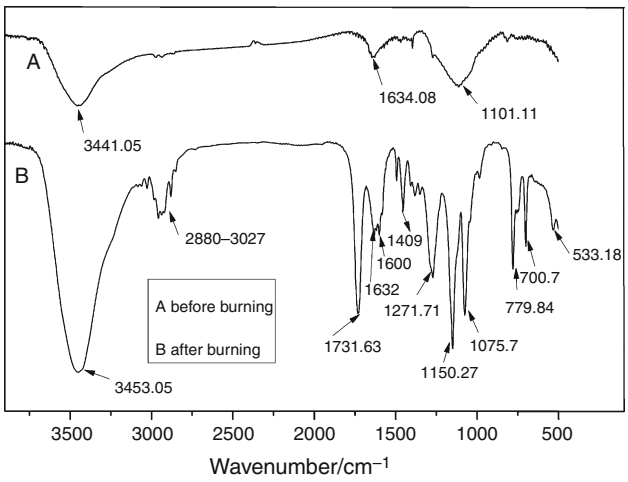

Fig. 6 FTIR spectrum of UPR-AlPi25 and the char after the LOI test

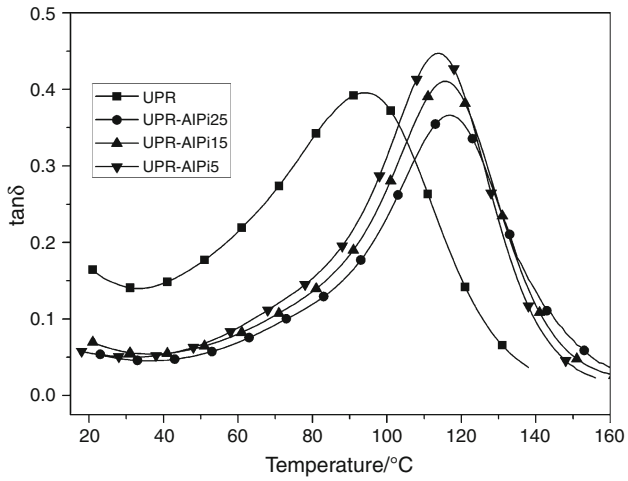

Fig. 7 DMA curves of UPR and UPR/AlPi composites

and the AlPi signals of diethylphosphinate anions are present at 1150, 1075 cm^{-1}(PO_2^-) [16], 1271 cm^{-1} (P=O) and 533 cm^{-1}(P–O). Compared with cured UPR-AlPi25, the residue at 3441.05 cm^{-1} has been assigned to the stretching mode of –OH from the P–OH group, which indicates the presence of alcohol groups in the char, and such a signal is compatible with the presence of organic phosphonic acid [23]. The aromatic ring or polyaromatics (1634 cm^{-1}) structure still existed in the residue. The absorption bands of aluminum phosphate derivatives (orthophosphate, pyrophosphate) (1101 cm^{-1}) were detected [28], giving positive evidence that when the temperature reached 700 °C, the phosphorus component in composites has changed its structure in the char layer. As a conclusion, it has been demonstrated that the AlPi degrades into aluminophosphates and some organic phosphonic acid (most probably ethyl phosphonic acid) [23] in the UPR.

Thermomechanical analysis of UPR/AlPi

To investigate the influence of AlPi in UPR, the glass transition temperature (T_g) of UPR/AlPi composites was determined by DMA. Figure 7 shows the DMA curves for neat UPR and various cured UPR/AlPi composites. The graph shows that the T_g of UPR/AlPi composites (114–116 °C) was higher than that of neat UPR (94.58 °C) and illustrates that AlPi can significantly improve the heat resistance of UPR. Table 4 gives the result of T_g. But with the increase in the dosage of AlPi, the T_g of UPR is almost not changed, and this is because a small amount of AlPi can reduce free volume of UPR, chain movement is blocked, while further increasing the dosage, free volume remains unchanged.

Compatibility and mechanical properties of UPR/AlPi composites

Comparing the tensile strength, flexural strength and modulus of UPR/AlPi composites, the results are given in Table 4. Incorporation of different content of fillers results in continuous reduction in flexural strength and tensile strength as the filler loading increases. However, flexural modulus of UPR/AlPi composites is higher than that of neat UPR. It may be caused by the restriction of the mobility and deformability of the matrix with the introduction of mechanical restraint [20]. Simultaneously, the higher stiffness (modulus) of these solid fillers than that of UPR matrix may also contribute to the above enhancement.

Figure 8 shows the flexural fracture surfaces of UPR/AlPi composites with different filler loading at magnification of

Table 4 Mechanical properties and heat resistance of UPR with different AlPi contents

Specimen	Mechanical properties			T_g/°C
	Tensile strength/MPa	Bending strength/MPa	Bending modulus/MPa	
UPR	58	73.3	2500	94.5
UPR-AlPi5	36.4	49.1	2923	114
UPR-AlPi15	26.2	45.2	3395	115.4
UPR-AlPi25	20.1	35.5	3532	116.5

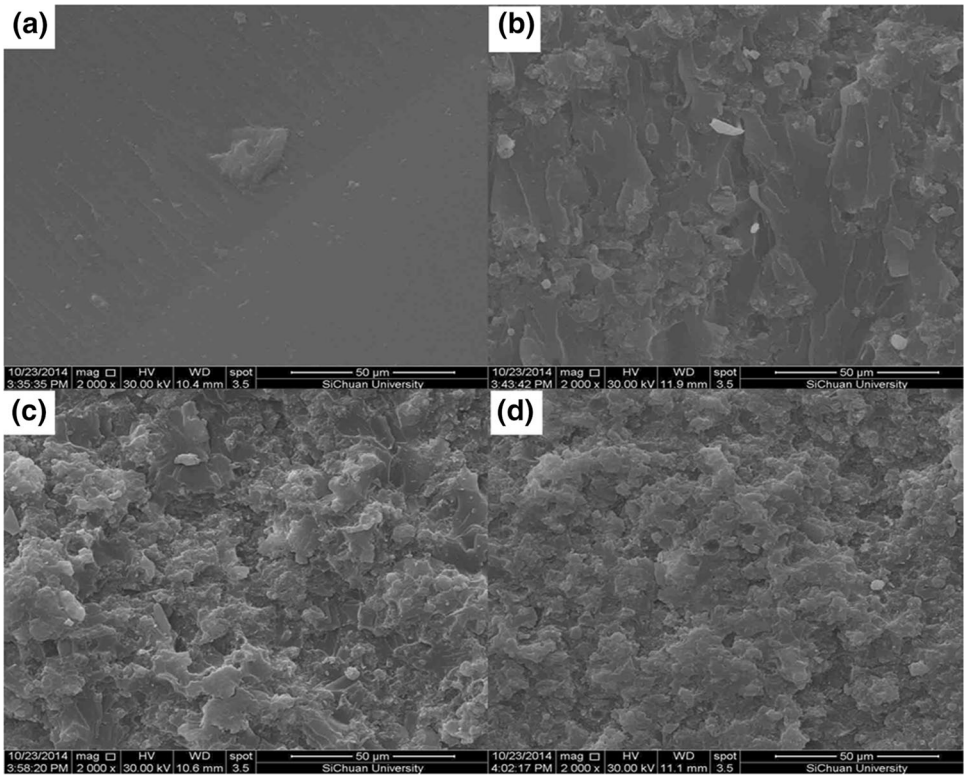

Fig. 8 SEM micrographs for fracture surfaces of UPR/AlPi composites (**a**, **b**, **c** and **d**) with different filler loading (m %): a: 0; b: 10; c: 15; and d: 25

2000×. It can be seen that the smooth cleavage surface of neat UPR shows many parallel lines, which is believed to be the crack-propagation direction. For low filler loading (10 %), as seen in Fig. 8b, the path of most of the cracks of composites is parallel to the crack-propagation direction, but not as obvious as pure resin and AlPi particles are dispersed uniformly. While the filler loading is beyond 10 % (Fig. 8c–d), the lines become smaller and denser, and the path of the crack tip is distorted and AlPi shows stacking and accumulation phenomenon. It indicates that higher filler content generates greater fracture areas through the development of rougher surfaces, which allows them to resist crack propagation. The distorted crack tips can cause deformation rack front, thus altering the path of the propagating crack [20].

Above phenomenon indicates the AlPi has good compatibility and strong interaction with the UPR matrix due to alkyls of AlPi. However, some aggregations and voids on the fracture surface are observed. The number and volume of aggregates and voids show upward trend with filler loading increasing. These aggregates and voids caused by the bad dispersion and bubble during samples processing because of the high viscosity of the system.

Conclusions

Flame retardancy of UPR can be improved by adding AlPi. When the AlPi concentration was 25 %, the LOI was 29.5, and a V-0 rating was obtained. TG curves demonstrated the interaction between AlPi and UPR could enhance the char-formation ability of the UPR/AlPi systems. The char residues could reach 15.74 % in N_2 and 20.83 % in air at 700 °C. FTIR showed that AlPi degrades into aluminophosphates and some organic phosphonic acid in the UPR. In SEM micrographs, a compact and tight char layer could be observed, which slowed heat and mass transfer between the gas and condensed phases. The DMA curves of various cured UPR/AlPi composites indicated AlPi can significantly improve the heat resistance of UPR. Incorporation of different content of fillers results in continuous reduction in flexural strength and tensile strength as the filler loading increases; however, flexural modulus of UPR/AlPi composites is higher than that of neat UPR.

Acknowledgements We would like to thank the generous supports by the following: National Natural Sciences Foundation of China,

Grant No. 50973066; the Experiment Center of Polymer Science and Engineering Academy, Sichuan University; Tiannan Zhou doctor; Xinhui Science and Technology co, LTD.

References

1. Tibiletti L, Longuet C, Ferry L, Coutelen P, Mas A, Robin JJ, et al. Thermal degradation and fire behaviour of unsaturated polyesters filled with metallic oxides. Polym Degrad Stab. 2011;96(1):67–75.
2. Baskaran R, Sarojadevi M, Vijayakumar CT. Unsaturated polyester nanocomposites filled with nano alumina. J Mater Sci. 2011;46(14):4864–71.
3. Penczek P, Czub P, Pielichowski J. Unsaturated polyester resins: chemistry and technology. Adv Polym Sci. 2005;184:1–95.
4. Vlad S, Oprea S, Stanciu A, Ciobanu C, Bulacovschi V. Polyesters based on unsaturated diols. Eur Polym J. 2000;36:1495–501.
5. Bai Z, Song L, Hu Y, Yuen RKK. Preparation, flame retardancy and thermal degradation of unsaturated polyester resin modified with a novel phosphorus containing acrylate. Ind Eng Chem Res. 2013;52:12855–64.
6. Liu YY, Wang SJ, Xiao M, Meng YZ. Halogen-free polymeric flame-retardants for common resins. Res J Chem Environ. 2007;11:84–103.
7. Chen MJ, Shao ZB, Wang XL, Chen L, Wang YZ. Halogen-free flame-retardant flexible polyurethane foam with a novel nitrogen-phosphorus flame retardant. Ind Eng Chem Res. 2012;51:9769–976.
8. Dai K, Song L, Yuen KK, Jiang SH, Pan HF, Hu YE. Enhanced properties of the incorporation of a novel reactive phosphorus- and sulfur-containing flame retardant monomer into unsaturated polyester resin. Ind Eng Chem Res. 2012;51:15918–26.
9. Pan LL, Li GY, Su YC, Lian JS. Fire retardant mechanism analysis between ammonium polyphosphate and triphenyl phosphate in unsaturated polyester resin. Polym Degrad Stab. 2012;97:1801–6.
10. Ricciardi MR, Antonucci V, Zarrelli M, Giordano M. Fire behavior and smoke emission of phosphate-based inorganic fire-retarded polyester resin. Fire Mater. 2012;36:203–15.
11. Horold S. Phosphorus flame retardants in thermoset resins. Polym Degrad Stab. 1999;64:427–31.
12. Klinkows C, Zang L, Doring M. DOPO-based flame retardants: synthesis and flame retardant efficiency in polymers. Mater China. 2013;32(3):144–58.
13. Fong KJ, Fu LK. Synthesis of hexa-allylamino-cyclotriphosphazene as a reactive fire retardant for unsaturated polyesters. J Appl Polym Sci. 2004;91(2):697–702.
14. Ma Z, Zhao W, Liu Y, et al. Synthesis and properties of intumescent phosphorus-containing flame-retardant polyesters. J Appl Polym Sci. 1997;63(12):1511–5.
15. M Doring, J Diederichs. Non-reactive-fillers in innovative flame retardants in E&E Applications. 2nd ed. Brussels Belgium pinfa. 2009. pp. 26–27.
16. Braun U, Schartel B, Fichera MA, Jager C. Flame retardancy mechanisms of aluminium phosphinate in combination with melamine cyanurate and zinc borate in glass-fibre-reinforced polyamide 6,6. Polym Degrad Stab. 2007;92:1528–45.
17. H Bauer, W Krause, M Sicken, N Weferling. US Patent. 7,420,007 (2008).
18. Levchik S, Weil ED. Polym Int. 2005;54:11.
19. Braun U, Bahr H, Sturm H, Schartel B. Polym Adv Technol. 2008;19:680.
20. X Liu, J Liu, S Cai. Comparative study of aluminum diethylphosphinate and aluminum methylethylphosphinate-filled epoxy flame-retardant composites. Polym Compos. 2012;33(6):918–26.
21. YL Liu, YC Chiu, CS Wu. Preparation of silicon-/phosphorous-containing epoxy resins from the fusion process to bring a synergistic effect on improving the resins' thermal stability and flame retardancy. J Appl Polym Sci. 2003;87(11):404–11.
22. F Samyn. Compréhension des procédés dignifugation du polyamide 6-Apport des nanocomposites aux systems retardateurs de flame phosphorés, PhD Thesis, Université de Lille1, 2007.
23. Duquesne Sophie, Fontaine Gaëlle, Cérin-Delaval Oriane, Gardelle Bastien, Tricot Grégory, Bourbigot Serge. Study of the thermal degradation of an aluminium phosphinate–aluminium trihydrate combination. Thermochim Acta. 2013;551:175–83.
24. Braun U, Schartel B. Flame retardancy mechanisms of AlPi in combination with melamine cyanurate in glass-fibre-reinforced poly(1,4-butylene terephthalate). Macromol. Mater Eng. 2008;293:206–17.
25. Lorenzetti A, Modesti M, Gallo E, Schartel B, Besco S, Roso M. Synthesis of phosphinated polyurethane foams with improved fire behaviour. Polym Degrad Stab. 2012;97(11):2364–9.
26. Samyn Fabienne, Bourbigot Serge. Thermal decomposition of flame retarded formulations PA6/aluminum phosphinate/melamine polyphosphate/organomodified clay: interactions between the constituents? Polym Degrad Stab. 2012;97:2217–30.
27. Braun U, Schartel B. Flame retardant mechanisms of red phosphorus and magnesium hydroxide in high impact polystyrene. Macromol Chem Phys. 2004;205:2185–96.
28. Si Mingming, Feng Jie, Hao Jianwei, Lishi Xu, Jianxin Du. Synergistic flame retardant effects and mechanisms of nano-Sb_2O_3 in combination with aluminum phosphinate in poly (ethylene terephthalate). Polym Degrad Stab. 2014;100:70–8.